SUSY SURVEY WITH INCLUSIVE MUON AND SAME-SIGN DIMUON ACCOMPANIED BY JETS AND MET WITH CMS*

Yu. Pakhotin, B. Scurlock, D. Acosta, P. Bartalini
R. Cavanaugh, A. Drozdetskiy, A. Korytov, K. Kotov
K. Matchev, G. Mitselmakher, M. Schmitt

Dept. of Physics, University of Florida
PO Box 118440, Gainesville, FL 32611-8440, USA

Generic signatures of supersymmetry with R-parity conservation include those of single isolated muons or like-sign isolated dimuon pairs, accompanied with energetic jets and missing transverse energy. The ability of CMS to discover supersymmetry with these signals is estimated for $10\,\mathrm{fb}^{-1}$ of data collected with the inclusive single-muon and dimuon high-level-trigger paths. The selection criteria are optimized and the systematic effects are studied for a single low-mass benchmark point of the constrained MSSM with $m_0 = 60\,\mathrm{GeV}/c^2$, $m_{1/2} = 250\,\mathrm{GeV}/c^2$, $\tan\beta = 10$, $A_0 = 0$ and $\mu > 0$. Discovery contours in the $(m_0, m_{1/2})$ plane are presented for integrated luminosities ranging from 1 to $100\,\mathrm{fb}^{-1}$.

PACS numbers: 12.60.Jv, 14.80.Ly

1. Introduction

Low energy supersymmetry is a promising candidate for new physics beyond the Standard Model (SM). The analysis presented in this paper is carried out in the framework of the CMSSM [1], also known as mSUGRA.

Small universal gaugino mass $m_{1/2}$ values have already been excluded by LEP searches [2]. While the Tevatron searches [3] do not have the sensitivity to extend LEP results in the CMSSM, the larger centre-of-mass energy and luminosities that will be made available at the LHC will allow a much larger domain of the parameter space to be covered. Owing to the ability of the CMS detector to identify and reconstruct muons with good efficiency [4], the analyses presented here address the topologies with either at least one

---

muon or a like-sign dimuon pair, accompanied with energetic jets and large transverse missing energy ($E_\mathrm{T}^\mathrm{miss}$). These signatures are experimentally clean when compared to that involving only jets and missing energy, and have the anticipated advantage of an efficient and well-understood trigger shortly after LHC start-up. The analysis with two same-sign muons is complementary to trilepton searches because it involves more diagrams [5–7]. Further, the two same-sign muons analysis is able to distinguish SUSY diagrams with good efficiency and purity by applying muon isolation and tight quality cuts [8–10].

All details of the full study, which forms the basis for the brief summary given in this paper, can be found in [11]. The results were obtained with the full CMS detector simulation and reconstruction software and included pile-up effects corresponding to an instantaneous luminosity of $2 \times 10^{33} \mathrm{cm}^{-2}\mathrm{s}^{-1}$.

2. Supersymmetry events simulation

The different parameters for all fully simulated SUSY points used in this work are listed in Table I.

TABLE I

Parameters of fully simulated and reconstructed SUSY benchmark points studied in this work.

	m_0 GeV/c^2	$m_{1/2}$ GeV/c^2	$\tan\beta$	A_0	μ	$\sigma_\mathtt{LO}$ pb	$N_\mathtt{Gen}$	L fb^{-1}
LM1	60	250	10	0	+	41.9	98250	2.3
LM2	185	350	35	0	+	7.4	93000	12.6
LM4	210	285	10	0	+	19	96500	5.1
LM5	230	360	10	0	+	6	84000	13.9
LM6	85	400	10	0	+	4	99250	24.6
LM7	3000	230	10	0	+	10.2	7500	0.7
LM8	500	300	10	−300	+	8.8	58250	6.6
LM10	3000	500	10	0	+	0.178	19750	110.7
HM1	180	850	10	0	+	0.052	80000	1538.5
HM2	350	800	35	0	+	0.068	28500	419.2

In addition to the fully simulated points, a scan of the $(m_0, m_{1/2})$ plane with a $(100\,\mathrm{GeV}/c^2,\ 100\,\mathrm{GeV}/c^2)$ grid is performed with a fast simulation, for $\tan\beta = 10$, $A_0 = 0$ and $\mu > 0$. For comparison, validation and efficiency calibration purposes, several of the benchmark samples of Table I are also processed with the fast simulation. The LM1 benchmark point is chosen for selection optimization in this study.

3. Standard Model (SM) backgrounds

Multi-jet QCD events do not intrinsically involve Feynman diagrams with final states similar to the topological signature required by this analysis. Owing to its enormous cross section ($\sigma_{jj} \sim 55\,\mathrm{mb}$), however, multi-jet events can produce configurations which are experimentally close. The number of multi-jet QCD events expected for integrated luminosity of $10\,\mathrm{fb}^{-1}$ is so large at small $\hat{p}_\mathrm{T}$ (defined as the transverse momentum of one of the two original hard scattered partons) that it is practically impossible to generate and simulate such a large amount of events. Consequently, events were generated almost uniformly in 21 $\hat{p}_\mathrm{T}$ bins.

Top pair production is another particularly important source of background, due to its modestly large cross section $\sigma_{t\bar{t}} \sim 490\,\mathrm{pb}$ (at leading order) and its intrinsic multi-jet, high missing transverse energy, and significant leptonic final state nature. A total of approximately 3.4 million $t\bar{t}$ events (corresponding to an equivalent integrated luminosity of $6.9\,\mathrm{fb}^{-1}$) were simulated and used in this analysis.

The production of single W and Z bosons is expected to be plentiful at the LHC due to their high cross sections, $\sigma_W \sim 1.2 \times 10^5\,\mathrm{pb}$ and $\sigma_Z \sim 3.3 \times 10^4\,\mathrm{pb}$ (at leading order). Because it is nearly impossible to generate and simulate all the needed events for integrated luminosity of $10\,\mathrm{fb}^{-1}$, the single-boson electroweak events were generated uniformly in 20 $\hat{p}_\mathrm{T}$ bins.

Diboson production, such as $WW + \mathrm{jets}$, $WZ + \mathrm{jets}$, and $ZZ + \mathrm{jets}$, also contributes as a source of background. Because of the additional weak vertex, the cross sections, while significant with respect to this study, are much less than for single-boson production: $\sigma_{WW} \sim 190\,\mathrm{pb}$, $\sigma_{WZ} \sim 27\,\mathrm{pb}$ and $\sigma_{ZZ} \sim 10\,\mathrm{pb}$ (at leading order).

4. Cuts optimization and search for the signal

The strategy of the analyses presented here involves searching for an excess in the number of events over the expected number from Standard Model backgrounds (*i.e.* a counting experiment) for an integrated luminosity of $10\,\mathrm{fb}^{-1}$. The algorithms to reconstruct the physical objects (muon, jets, *etc.*) as well as their identification at the online and offline levels are described in Ref. [4].

This work uses event samples selected by the inclusive single-muon and the dimuon triggers, which are relatively clean and easier to understand than other triggers based purely on jets and $E_\mathrm{T}^\mathrm{miss}$.

In the single-muon analysis, the leading muon is required to be reconstructed with a momentum in excess of $30\,\mathrm{GeV}/c$, and both muons must be reconstructed with a p_T in excess of $10\,\mathrm{GeV}/c$ in the dimuon analysis. These cuts ensure the muon candidates are reconstructed with good efficiency, and with a momentum well above the trigger thresholds.

In addition, muons from prompt sparticle decays are best recognized by the requirement that the χ^2 of the global trajectory fit be smaller than 3.0 per degree of freedom, and the total number of hits associated to the muon track exceed 12. These quality cuts are $\sim 100\%$ efficient for prompt muons, but allow a fair fraction of fake muons or muons from long-lived particle ($\pi^{\pm}$, $K^{\pm}$) decays to be rejected.

Further, the leading muon (single-muon analysis) and the two leading muons (dimuon analysis) are required to be isolated with less than $10\,\mathrm{GeV}$ in a cone of radius 0.3 around the muon direction. These isolation requirements reject many of the muons, from b- or c-quark semi-leptonic decays, not rejected by the aforementioned quality cuts.

Events from SUSY tend to have jet multiplicities higher than those of the SM events. Both studies thus require at least 3 jets. The three leading jets must each have an E_T of at least $50\,\mathrm{GeV}$ which guarantees that jets are reconstructed with good efficiency. No quality pre-selection requirements are made on the $E_\mathrm{T}^{\mathrm{miss}}$.

Signal and background can be disentangled with a series of cuts on observables that carry some discrimination power. A genetic algorithm tool, known as GARCON [12], is used to search a multi-dimensional space of cuts, with the aim of maximizing the significance for potential discovery.

In the single-muon analysis, the primary features which are exploited to separate signal from the remaining backgrounds are the distinctly harder jets and $E_\mathrm{T}^{\mathrm{miss}}$ spectra, the centrality of the leading jets, as well as the azimuthal angles between the $E_\mathrm{T}^{\mathrm{miss}}$ vector and jets. No additional tightening of the muon p_T cut is made when applying the final selection cuts.

TABLE II

All selection cuts as applied in the inclusive single-muon analysis.

		Cut criteria	
Pre-selection	number of muons ≥ 1 "AND" p_T	$>$	$30\,\mathrm{GeV}/c$
	μ calo. iso. $(R = 0.3)$ E_T	$<$	$10\,\mathrm{GeV}$
	number of jets ≥ 3 "AND" E_T	$>$	$50\,\mathrm{GeV}$
Selection	leading jet (Jet1) $E_\mathrm{T}^{\mathrm{Jet1}}$	$>$	$440\,\mathrm{GeV}$
	next-to-leading jet (Jet2) $E_\mathrm{T}^{\mathrm{Jet2}}$	$>$	$440\,\mathrm{GeV}$
	$|\eta^{\mathrm{Jet1}}| < 1.9$, $|\eta^{\mathrm{Jet2}}| < 1.5$, $|\eta^{\mathrm{Jet3}}|$	$<$	3.0
	$-1 < \cos\left[\Delta\phi(\mathrm{Jet1},\ \mathrm{Jet2})\right]$	$<$	0.2
	$-0.95 < \cos\left[\Delta\phi(E_\mathrm{T}^{\mathrm{miss}},\ \mathrm{Jet1})\right]$	$<$	0.3
	$-1 < \cos\left[\Delta\phi(E_\mathrm{T}^{\mathrm{miss}},\ \mathrm{Jet2})\right]$	$<$	0.85
	$E_\mathrm{T}^{\mathrm{miss}}$	$>$	$130\,\mathrm{GeV}$
Trigger	single-μ "OR" di-μ	$=$	"Accept"

A total of eleven variables is provided as input to the genetic algorithm and the results of that search are displayed in Table II. Background contamination into the signal region is estimated to be 2.5 ± 0.5 SM events. The inclusive single-muon analysis re-optimizes the cuts to select the HM1 point assuming higher integrated luminosity.

In the dimuon analysis, there is a large $E_\mathrm{T}^\mathrm{miss}$ excess for signal events compared with background. The E_T spectra for the three leading jets in SUSY events tend to be significantly harder than in SM events. No additional tightening of the muons p_T cuts is made when applying the final selection cuts. The leading muon, for both signal and background, already tends to be isolated and hence does not discriminate well. However, the second leading muon tends to be more isolated in the signal than in the background.

A total of nine variables are used in the genetic algorithm. Table III provides a summary of the final cuts. The total number of remaining SM background events is estimated to be 1.5 ± 0.3 and comes solely from $t\bar{t}$ production. The muon isolation requirements are a key factor in selecting events corresponding to SUSY diagrams with prompt muons. Indeed, the dimuon analysis selects such diagrams with $\sim 65\%$ efficiency and over $\sim 90\%$ purity.

TABLE III

All selection cuts as applied in the dimuon analysis.

	Cut criteria		
Pre-selection	2 same-sign muons with p_T	$>$	$10\,\mathrm{GeV}/c$
	number of hits per μ track ≥ 13 and χ^2_μ	$<$	3
	isolation $\mathtt{Iso}_{\mu 1} < 10\,\mathrm{GeV}$ and $\mathtt{Iso}_{\mu 2}$	$<$	$6\,\mathrm{GeV}$
	number of jets ≥ 3 with E_T	$>$	$50\,\mathrm{GeV}$
Selection	next-to-next-to-leading jet $E_\mathrm{T}^\mathrm{Jet3}$	$>$	$55\,\mathrm{GeV}$
	next-to-leading jet $E_\mathrm{T}^\mathrm{Jet2}$	$>$	$130\,\mathrm{GeV}$
	leading jet $E_\mathrm{T}^\mathrm{Jet1}$	$>$	$175\,\mathrm{GeV}$
	$E_\mathrm{T}^\mathrm{miss}$	$>$	$200\,\mathrm{GeV}$
Trigger	di-μ	$=$	"Accept"

5. Systematic uncertainties

By the time $10\,\mathrm{fb}^{-1}$ of integrated luminosity is gathered, the CMS Jet Energy Scale is expected to be calibrated at the level of 3% via a W mass constraint in semi-leptonic $t\bar{t}$ events. Accordingly, a scaling is applied to all reconstructed jet E_T's and the $E_\mathrm{T}^\mathrm{miss}$.

With $10\,\mathrm{fb}^{-1}$ of integrated luminosity, the CMS Jet Energy Resolution is expected to be known to within 10% via dijet balancing. Accordingly, a Gaussian smearing is applied to all reconstructed jet E_T's and the $E_\mathrm{T}^{\mathrm{miss}}$, event by event.

The systematic uncertainty in the muon p_T, due to uncertainties in the magnetic field translates to a negligible uncertainty in the efficiency to trigger and reconstruct muons in these analyses. The systematic uncertainty on the rate of backgrounds passing the selection cuts due to fake muons is also estimated to be negligible.

Reference [4] indicates that once approximately $10\,\mathrm{fb}^{-1}$ of integrated luminosity has been collected by CMS, the uncertainty in measuring that integrated luminosity is estimated to be $\sim 5\%$.

The acceptance of high E_T ISR/FSR jets as generated by PYTHIA [13] can be significantly underestimated in these studies. The full matrix element calculation (obtained via CompHEP [14], for example) increases the relative acceptance of $t\bar{t}+1$ jet events by approximately 10%, which is taken as a systematic uncertainty. In addition to ISR/FSR, other theoretical effects involving (1) pile-up, (2) underlying event and (3) parton distribution function (PDF) uncertainties are each assumed to be at the level of 5%.

Table IV shows the final list of all systematic uncertainties considered in this analysis.

TABLE IV

List of systematic uncertainties considered in this work.

Systematic	Uncertainty ($\delta N/N$)	
	single-muon	dimuon
Jet energy scale	10%	15%
Jet energy resolution	5%	10%
Luminosity	5%	5%
Theory	13%	13%
Background total	18%	23%

6. Results

This work demonstrates that the low mass CMSSM benchmark point, LM1, could be easily observable before $1\,\mathrm{fb}^{-1}$ of data has been collected, including systematic uncertainties. The optimized cuts are used in a scan across the $(m_0, m_{1/2})$ plane, and the results indicate that most of the low mass region for $\tan\beta = 10$, $A_0 = 0$ and $\mu > 0$ can be observed up to mass scales of $\sim 1.5\,\mathrm{TeV}/c^2$, including systematic effects. Fig. 1 shows the 5σ reach contours for both analyses (including systematic uncertainties)
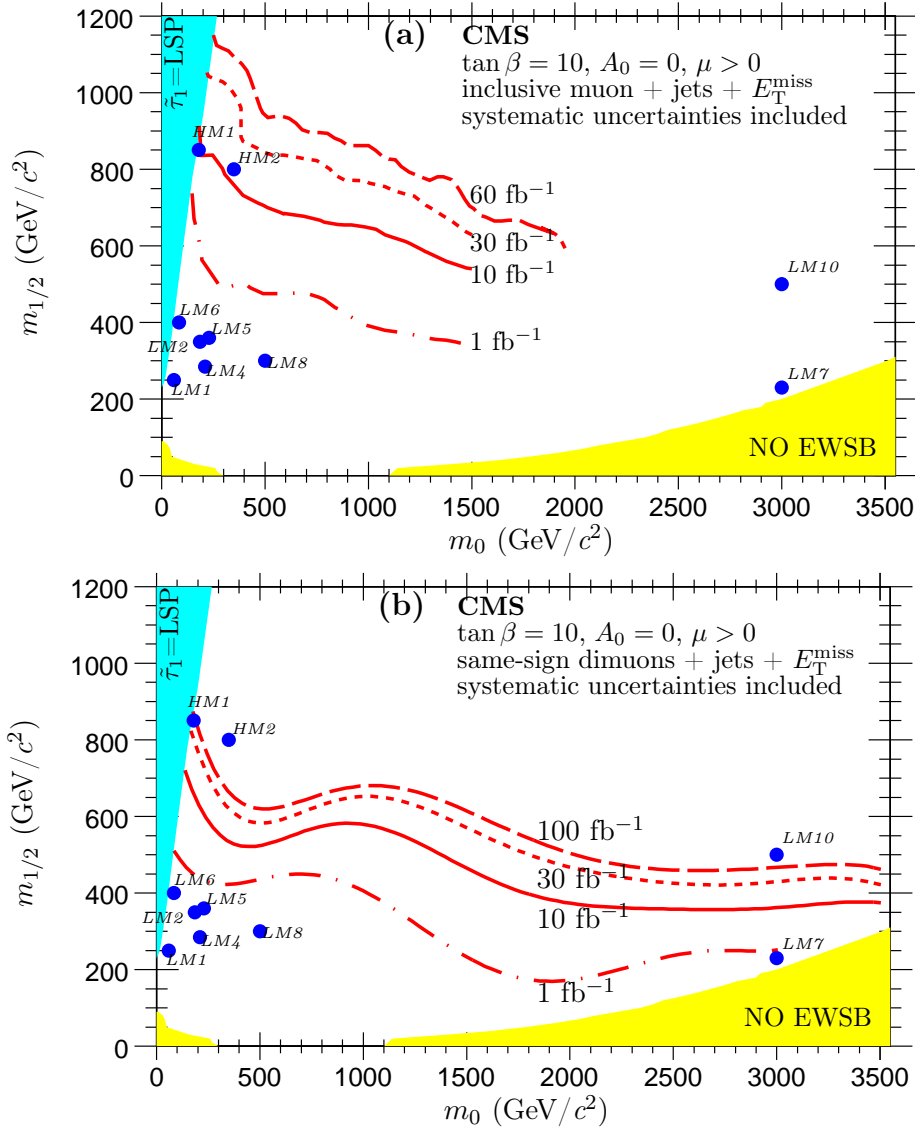
Fig. 1. Plot (a) displays the inclusive single-muon 5σ CMS reach contours in the $(m_0, m_{1/2})$ plane for integrated luminosity of $1\,\mathrm{fb}^{-1}, 10\,\mathrm{fb}^{-1}, 30\,\mathrm{fb}^{-1}, 60\,\mathrm{fb}^{-1}$ including systematic uncertainties; the reach curves for $1\,\mathrm{fb}^{-1}, 10\,\mathrm{fb}^{-1}$ are optimized to select the point LM1; the reach curves for $30\,\mathrm{fb}^{-1}, 60\,\mathrm{fb}^{-1}$ are optimized to select the point HM1. Plot (b) displays the dimuon 5σ CMS reach contours in the $(m_0, m_{1/2})$ plane for integrated luminosity of $1\,\mathrm{fb}^{-1}, 10\,\mathrm{fb}^{-1}, 30\,\mathrm{fb}^{-1}, 100\,\mathrm{fb}^{-1}$ including systematic uncertainties, collectively optimized to select all benchmark points. Both reach contour plots assume fixed CMSSM parameters of $\tan\beta = 10$, $A_0 = 0$, $\mu > 0$.

in the CMSSM $(m_0, m_{1/2})$ plane, assuming integrated luminosity of $10\,\mathrm{fb}^{-1}$. With $30\,\mathrm{fb}^{-1}$ of data, the high mass SUSY benchmark points become interesting for possible discovery and with $60\,\mathrm{fb}^{-1}$ of data, SUSY mass scales beyond $2\,\mathrm{TeV}/c^2$ can be probed, including systematic uncertainties.

REFERENCES

[1] S. Abel, *et al.*, `hep-ph/0003154`.

[2] LEPSUSYWG, ALEPH, DELPHI, L3 and OPAL experiments, "LEP2 SUSY Working Group Web Page", `http://lepsusy.web.cern.ch/lepsusy/`.

[3] V. Abazov, *et al.*, (D∅ Collaboration), *Phys. Lett.* **B638**, 119 (2006).

[4] CMS Collaboration, CERN/LHCC 2006-001, (2006).

[5] H. Baer *et al., Phys. Rev.* **D41**, 42 (1990).

[6] R. Barnett *et al.*, *Phys. Lett.* **B315**, 349 (1993).

[7] K. Matchev, D. Pierce, `hep-ph/9904282`.

[8] J. Done, FNAL-Thesis-1999-13, (1999).

[9] M. Worcester, FNAL-Thesis-2004-05, (2004).

[10] A. Yurkewicz, FNAL-Thesis-2004-11, (2004).

[11] Yu. Pakhotin, B. Scurlock, *et al.*, CMS Note 2006/134, (2006).

[12] S. Abdullin, *et al.*, `hep-ph/0605143`.

[13] T. Sjostrand, S. Mrenna, P. Skands, `hep-ph/0603175`.

[14] A. Pukhov, *et al.*, `hep-ph/9908288`.